and J. E. Mercereau for suggesting the proposed experimental test of our assumption.

---

*Work supported in part by a Frederick Gardner Cottrell Grant-In-Aid, from the Research Corporation, New York.

†Alfred P. Sloan Research Fellow.

[1]See, e.g., L. D. Landau and E. M. Lifshitz, *Fluid Mechanics* (Pergamon, New York, 1959), p. 510 *et seq*.

[2]V. M. Kontorovich, Zh. Eksperim. i Teor. Fiz. 30, 805 (1956) [Soviet Phys. JETP 3, 770 (1956)].

[3]W. E. Keller, Phys. Rev. Letters 24, 569 (1970).

[4]E. R. Huggins, Phys. Rev. Letters 24, 573 (1970).

[5]E. R. Huggins, Phys. Rev. Letters 24, 699 (1970). Also, W. E. Keller and E. R. Huggins, private communications.

[6]It has previously been pointed out that Eq. (2) is inappropriate for very thin, i.e., unsaturated films. See D. L. Goodstein, Phys. Rev. 183, 327 (1969). Here we are contending that it is unacceptable even for the relatively thick, i.e., saturated films investigated by Keller.

[7]The detailed analysis will be presented elsewhere.

[8]See e.g., T. L. Hill, J. Chem. Phys. 17, 520 (1949); L. Meyer, Phys. Rev. 97, 22 (1955).

[9]J. F. Allan and A. D. Misener, Proc. Cambridge Phil. Soc. 34, 299 (1938).

[10]K. R. Atkins, Can. J. Phys. 31, 1165 (1953); K. R. Atkins and Y. Narahara, Phys. Rev. 138, A437 (1965).

[11]D. S. Hyman, M. O. Scully, and A. Widom, Phys. Rev. 186, 231 (1969).

[12]W. D. Johnston and J. G. King, Phys. Rev. Letters 16, 1191 (1966).

[13]A correction is necessary due to the van der Waals potential in the gas. With this correction, our prediction for saturated stationary films is the same as that made by the authors of Ref. 11. Our reasoning has been partly based on their theory.

[14]For a review, see D. M. Young and A. D. Crowell, *Physical Adsorption of Gases* (Butterworths, London, 1962), p. 167 *et seq*.

VOLTAGE-INDUCED VORTICITY AND OPTICAL FOCUSING IN LIQUID CRYSTALS

P. Andrew Penz
Scientific Research Staff, Ford Motor Company, Dearborn, Michigan 48121
(Received 27 April 1970)

We have observed that liquid crystals of the *p*-azoxyanisole type exhibit macroscopic rotational motion above a threshold voltage. The vortex motion of the birefringent liquid results in a lattice of cylindrical lenses whose focal lengths are voltage variable. These experiments are in excellent agreement with the dynamic predictions of the continuum theory.

The effects of electric fields on the optical properties of liquid crystals have received considerable attention recently because of their display applications.[1] We report experiments involving the dynamic scattering mode (DSM)[2] which is observed in certain nematic liquid crystals. Electric fields applied to *p*-azoxyanisole (PAA) induce a visible pattern, referred to as a domain pattern.[3] Our experiments are the first to demonstrate that the visible pattern results from the formation of liquid crystal lenses concomitant with cells of liquid rotation. The experiments also provide the first complete experimental description of the threshold voltage for vortex formation. We believe that these observations give conclusive verification of Helfrich's conduction-induced-alignment theory.[4]

We have used the customary experimental configuration in which the liquid crystal is held in a parallel plate capacitor with transparent Nesatron electrodes. The sample thickness d was held fixed by Teflon spacers. PAA was purchased commerically and used without further purification. The sample was viewed with a Leitz polarizing microscope in the transmission mode. A hot stage regulated the temperature in the liquid crystal region, 116° to 136°C for PAA. Both Nesatron surfaces were wiped vigorously along a single direction in order to promote a uniform alignment of the order director $\vec{S}$.[5] In the continuum theory of liquid crystals, $\vec{S}$ is a unit vector pointing in the average direction of molecular order in a fluid volume element.[6] An orthogonal coordinate system is established by defining the x direction as the rubbing direction and the z direction as the axis of the applied electric field and the gravitational field. The domain lines can be observed using either dc or audio-frequency ac electric fields. We have found that the electrical and optical properties are much more reproducible when ac fields are employed. dc fields may unnecessarily complicate the experiments because of impurity-ion polarization and electrochemical reactions at the electrodes. The

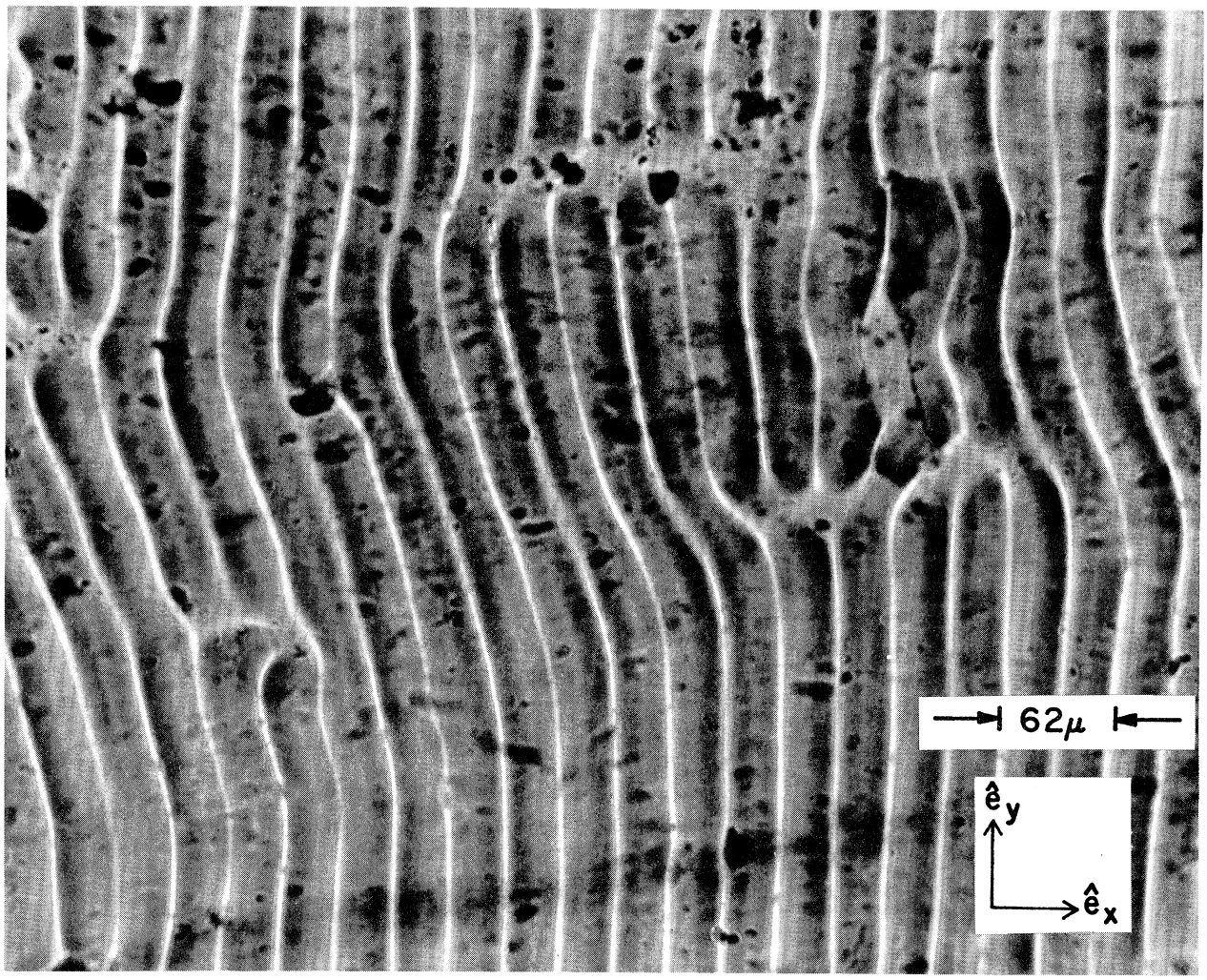

FIG. 1. Domain pattern in PAA observed in transmission. A 38-μm sample has been subjected to a 7.8-V driving voltage at 130°C. The rubbing direction (x) is horizontal and the voltage is applied perpendicular to the page (z). The microscope is focused near the top electrode and has a ± 10-μm depth of focus. The top set of bright domain lines are visible and have a spacing of 31 μm or $\frac{1}{2}\lambda_t$. When the microscope is focused at the sample bottom, another set of bright domain lines is visible. Several dislocations in the domain pattern are visible as are many particles of dust, some badly out of focus.

experiments reported below were performed in the neighborhood of 100 Hz and the voltages are given in rms volts. No frequency dependence was noted from 50 to 500 Hz. The typical resistivity of our samples in the liquid crystal region was 10^9 Ω cm at 100 Hz.

Figure 1 shows a transmission photograph of the domain pattern at 7.8 V and 130°C for a sample thickness $d = 38 \pm 1$ μm. The top conducting surface is in focus. The incident light was polarized in the x direction; an analyzer was not used. The bright lines form a pattern generally parallel to the y direction and are known as domain lines. The lattice pattern is not completely regular as indicated by the visible dislocations. This particular pattern first became visible at a voltage of 6.8 ± 0.2 V and had a periodicity in the x direction of $\lambda_t = 62 \pm 2$ μm. Investigation at slightly different depths reveals that the pattern repeats every other line as might be concluded from Fig. 1.

Previous experiments[7,8] have shown that the voltage for the first observation of the domain pattern is insensitive to sample thickness, leading to the term threshold voltage. It has also been found that the ratio $\lambda_t/2d$ is not sensitive

to d.[3] While 30% sample-to-sample variation in both V_t and $\lambda_t/2d$ is seen, we have found that the product $V_c = V_t\lambda_t/2d$ is not sample dependent and may be called a characteristic voltage. For the sample pictured in Fig. 1, $V_c = 5.5 \pm 0.2$ V which is typical of the V_c's observed for other samples. We have found that λ_t is independent of voltage up to 3 V above threshold and may thus be referred to as a threshold wavelength. The domain pattern is stationary on a time scale of several seconds up to 2 V above threshold. As the voltage is raised further, the pattern becomes increasingly dynamic in the x-y plane, and many more dislocations appear. This turbulence is the reason for the DSM name. This paper will be principally concerned with the static pattern at threshold. Previous experiments have shown that the domain pattern is not visible when the incident light is completely polarized in the y direction.[9] It should be emphasized, however, that the pattern is clearly visible in unpolarized light.

Visual investigation of the domain pattern reveals two features which have not been previously reported. First there are two sets of bright domain lines. One set appears above the midplane ($z = 0$) of the sample and the other below. The idealized positions of the domain lines are indicated schematically in Fig. 2(a). The figure shows a cross section of the capacitor of thickness $d = 2r$. The lines above the sample midplane are in focus at $(x, z) = ((n + \frac{1}{4})\lambda_t, N'(V)r)$ and the bottom lines have $(x, z) = (\frac{1}{2}n\lambda_t, -N(V)r)$, where n is an integer. N and N' are approximately equal and depend on voltage. At threshold a typical value of N is 4, i.e., the lines are observed to lie outside the liquid crystal sample volume. The observation of bright lines exterior to the sample implies that the light is being focused. N and N' decrease with increasing voltage and saturate at approximately 1 at 3 V above threshold. The liquid crystal appears to act as a lattice of cylindrical lenses producing real and virtual images of the microscope lamp source at a voltage-variable focal length.[10] Note that the real and virtual images are separated by $\frac{1}{4}\lambda_t$ on the x axis.

The second important feature is the direct observation of fluid rotation by means of tracer particles inside the sample. Dust particles are inevitably introduced into the sample during preparation. Typical particle diameters of 5 μm are easily resolvable at ×100 magnification. Below threshold voltage the dust is stationary. At

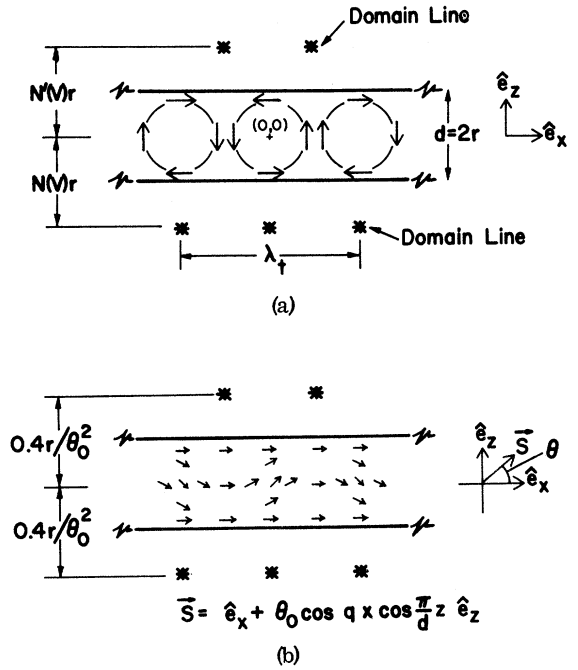

FIG. 2. Idealized spatial order. (a) A cross section of the fluid vortex pattern is observed by tracer particle motion. The streamlines are approximated by circles in cells of width $\frac{1}{2}\lambda_t$. The vorticity is antiparallel in adjacent cells. Real images appear a distance $N'(V)r$ above the outermost portion of a cell, the light being incident from below. Virtual images appear a distance $N(V)r$ below the rotation centers. The origin of the coordinate system is at (0,0). (b) The orientation of $\vec{S}$ as deduced from the shear flow in (a). The orientation of $\vec{S}$ is constant on concentric contours. The optical path length through the center of a cell is a minimum ($n_\parallel < n_\perp$). On the edge of a cell the optical path is maximum. The focal length of the cylindrical lens system is $f = 0.4r/\theta_0^2$ for $rq = 1.8$.

threshold the particles begin a well-defined oscillatory motion which is closely correlated with the domain pattern. By observing the particles move in and out of focus, it can readily be determined that the orbits are roughly circular and are in planes perpendicular to the y direction. Figure 2(a) shows the location of the idealized streamlines with respect to the domain lines. The particles revolve between the upper ($z > 0$) domain lines which thus define the fluid rotation cells. In adjacent cells, the vorticities are observed to be antiparallel. The observed particle orbits have steady-state diameters of approximately $\frac{1}{2}\lambda_t$. Oscillation periods at threshold range from several seconds for $d = 125$ μm to fractions of a second for $d = 38$ μm. It is experimentally clear that at threshold the liquid crystal

transforms from a static state into a highly ordered rotational state with vorticity in the $\pm y$ direction. Coherent vortex motion does not extend indefinitely in the y direction. The ends of the rotational cells are found to coincide with dislocations in the visible pattern as shown in Fig. 1. The focusing properties and the fluid rotation were not found to be temperature sensitive in the nematic region.

Helfrich has shown that the anisotropic conductivity associated with the director can lead to a flow instability in liquid crystals of the PAA type.[4] For PAA in the nematic phase, the conductivity parallel to $\vec{S}$ is 50% larger than the perpendicular conductivity. Helfrich employed the continuum model and considered the stability of a small-angle distortion θ_0 in the director, $\vec{S}=\hat{e}_x+\hat{e}_z\theta_0\times\cos qx$, where q is $2\pi/\lambda$. The space charge associated with this distortion leads to shear flow $\partial v_z/\partial x$ where v_z is the z component of the velocity. Shear flow is known to orient $\vec{S}$, in this case into the z direction.[11] The theory predicts that a distortion of wavelength λ will become unstable at a voltage $V=V_c'(2d/\lambda)$.[12] V_c' is a number which results from a combination of liquid crystal constants and is thus a characteristic of the bulk material. For PAA these constants have been measured, and $V_c'=5.3$ V at 130°C.

It is clear that the threshold voltage for instability V_t will result from the maximum wavelength λ_t. Consideration of the boundary value problem at the capacitor faces lead to a predicition that $\lambda_t\sim 2d$.[4] Williams's original experiments indicated that the threshold wavelength does increase with sample thickness such that $\lambda_t=0.6\times 2d$.[3] Since λ_t increases as $2d$, the voltage for the initial instability V_t is predicted to be roughly independent of thickness, as has been observed.[7,8] Clearly the theoretical number V_c' is to be identified with the experimental number V_c. V_c, involving V_t, λ_t, and d, was reported above to be 5.5 ± 0.2 V. This is within experimental uncertainty of the theoretical characteristic voltage of 5.3 V. Theoretical consideration of the boundary-value problem also leads to the prediction of a vortex-type motion at threshold, the vorticity in one cell antiparallel to that in the two adjacent cells.[13] This prediction is in agreement with the observed fluid motion diagrammed in Fig. 2(a). The theory predicts solid-body fluid rotation near the center of the circulation, i.e., velocity proportional to radius. This is consistent with experimental observations.

It is reasonable to refine the original assumption for the distortion in $\vec{S}$ to include the effects of the boundary at $z=\pm\frac{1}{2}d$: $\vec{S}=\hat{e}_x+\hat{e}_z\theta_0\cos qx\times\cos(\pi z/d)$. This distortion is diagrammed in Fig. 2(b). The orientation follows directly from consideration of the shear flow shown in Fig. 2(a). Fluid elements move on contours which have a common center. On each contour the director has a constant orientation which is maximum at the center and decreases toward the outside. This pattern has obvious potential for focusing. Using the small-angle approximation, the z component of the index of refraction is $n_z=n_\perp+(n_\parallel-n_\perp)\theta_0^2\cos^2qx\cos^2\pi z/d$. $n_\parallel$ and $n_\perp$ are the indices of refraction parallel and perpendicular to $\vec{S}$. Calculation of the optical path length $\int n_z dz$ shows that a diverging lens should exist at $x=0$; a virtual image below the sample will result. At $x=\pm\frac{1}{4}\lambda$, a converging lens will produce a real image above the sample. The focal lengths of both these lenses have the magnitudes $f=[(n_\parallel-n_\perp)\theta_0^2qd^2]^{-1}$. Using the appropriate values[14] of $n_\parallel$ and $n_\perp$ and $qr=1.8$ which was observed for Fig. 1, we obtain $f=0.4r/\theta_0^2$. The observed focal lengths of $4r$ at voltages slightly above threshold can be interpreted as $\theta_0=18°$. Independent evidence on the change in sample resistance near V_t is consistent with this value of θ_0.[7] Clearly the decrease of f with increasing voltage above threshold can be interpreted as an increase in the amplitude of the distortion θ_0. The maximum possible distortion is $\vec{S}=(\hat{e}_x+\hat{e}_z)/\sqrt{2}$, since at this 45° angle the space charge producing the distortion changes sign. The minimum focal length to be expected using this model is $f=0.8r$ which is in good agreement with the observation that the influence of the voltage on the focal length saturates at $f\sim 1r$. Since the model involves distortion perpendicular to the y direction, light polarized in the y direction should not be focused. This is also in agreement with experiment.

The conduction-induced-vortex model has been shown to explain the stationary vortex pattern near threshold voltage. It also gives a plausible explanation for the turbulence which results as the voltage is increased above threshold. Vortex motion is not possible below a threshold voltage V_t at a maximum wavelength λ_t. As the voltage is further increased, however, shorter wavelength vortex patterns become unstable. The hydrodynamic interaction of vortex patterns of different wavelengths will be very complicated, but there is a strong potential for the development of turbulence. Since the director $\vec{S}$ need not join smoothly between vortices of different

λ, large-angle scattering of incident light is to be expected. We have observed that shorter wavelength patterns do exist at higher voltages. They also have large-angle scattering properties and are consequently important for the display application of the DSM.

In conclusion, we have observed a voltage-induced liquid rotation in PAA. Concurrent with this rotation is a focusing by the birefringent liquid crystal. The value of the characteristic voltage, the liquid rotation, and the quantitative focusing properties are all predicted by a conduction-induced-alignment model. We believe that this agreement of experiment and theory constitutes a verification of the theory. The experiments reveal that the threshold optical properties of PAA are not the result of random fluctuations as might be implied by the name dynamic scattering mode. Underlying the turbulence at higher voltages is a macroscopically oriented rotational state.

The author wishes to acknowledge many stimulating and fruitful discussions with T. K. Hunt. The author also wishes to thank L. Bartosiewicz for the use of his microscope and helpful discussions.

Note added in proof.—It has been pointed out to the author that electric-field-induced mass transfer has been observed previously in liquid dielectrics and liquid crystals.[15]

[1]G. H. Heilmeier, Sci. Am. 222, No. 4, 100 (1970).
[2]G. H. Heilmeier, L. A. Zanoni, and L. A. Barton, Proc. IEEE 56, 1152 (1968).
[3]R. Williams, J. Chem. Phys. 39, 384 (1963).
[4]W. Helfrich, J. Chem. Phys. 51, 4092 (1969).
[5]P. Chatelain, Acta Cryst. 1, 315 (1948).
[6]See, e.g., I. G. Chistyakov, Usp. Fiz. Nauk 89, 563 (1966) [Soviet Phys. Usp 9, 551 (1967)].
[7]P. A. Penz, Bull. Am. Phys. Soc. 15, 59 (1970).
[8]G. Assouline and E. Leiba, J. Phys. (Paris) 30, C4-109 (1969).
[9]W. Helfrich, J. Chem. Phys. 51, 2755 (1969).
[10]Reference 9 mentions a possible focusing which is not in agreement with the number of images observed per wavelength.
[11]W. Helfrich, J. Chem. Phys. 50, 100 (1969).
[12]The basic physical mechanisms are easily understood. Because of the tensor conductivity, the distortion leads to current flowing in the x direction when the electric field is first applied. Space charge will build up to reduce the transverse current to zero. The space charge will be extremum at $x=\pm\frac{1}{4}\lambda$. The combined effect of shear stress due to the applied field acting on the space charge and the hydrodynamic viscosity will produce fluid motion parallel to the z axis. v_z is extremum at $x=\pm\frac{1}{4}\lambda$ and $\partial v_z/\partial x$ is extremum at $x=0$. The director-orienting torque due to shear flow is maximum at the distortion maximum. The possibility for instability is apparent.
[13]Fluid moving in the $+z$ direction will be deflected by the capacitor plate. At the position of velocity extreme, $x=\frac{1}{4}\lambda$, some fluid will be deflected in the $+x$ direction and some fluid in the $-x$ direction. Since fluid mass must be conserved, rotational cells of width $\frac{1}{2}\lambda$ will be set up, adjacent cells having antiparallel vorticity.
[14]P. Chatelain, Bull. Soc. Franc. Mineral. Crist. 60, 280 (1937).
[15]W. H. Middendorf and G. H. Brown, Trans. Am. Inst. Elec. Engrs. 77III, 795 (1958).

LEE-YANG THEOREM AND THE GRIFFITHS INEQUALITY FOR THE ANISOTROPIC HEISENBERG FERROMAGNET

Taro Asano
Institute for Graphics, College of General Education, University of Tokyo, Tokyo, Japan
(Received 29 April 1970)

It is shown that the zeros of the partition function of the anisotropic Heisenberg ferromagnet locate on the unit circle in the complex "fugacity" plane, and all the spin correlation functions are non-negative when no external magnetic field is present.

The Lee-Yang theorem,[1-3] which states that all the zeros of the partition function of the Ising ferromagnets locate on the unit circle in the complex "fugacity" plane, has been expected to hold for the Heisenberg ferromagnet and has been partly proved for special cases.[4] Here this theorem is proven generally. Let H be the Hamiltonian of the anisotropic Heisenberg ferromagnet with spin $\frac{1}{2}$ of n spins,

$$H=-\sum_{n\geq i>j\geq 1} J_{ij}H_{ij}, \tag{1}$$

where

$$H_{ij}=\tfrac{1}{2}(\sigma_{iz}\sigma_{jz}-1)+\tfrac{1}{2}\gamma_{ij}(\sigma_{ix}\sigma_{jx}+\sigma_{iy}\sigma_{jy}). \tag{2}$$

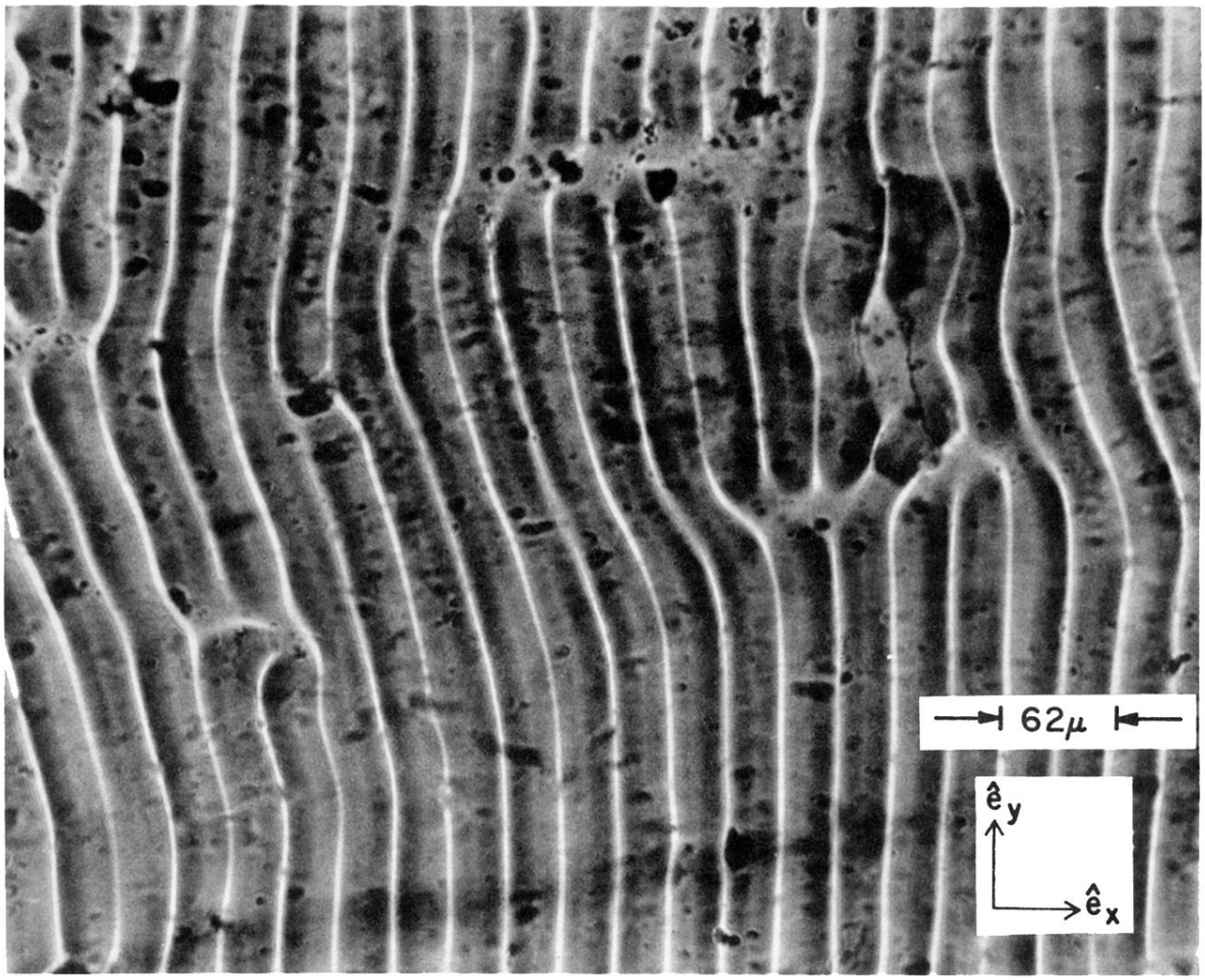

FIG. 1. Domain pattern in PAA observed in transmission. A 38-μm sample has been subjected to a 7.8-V driving voltage at 130°C. The rubbing direction (x) is horizontal and the voltage is applied perpendicular to the page (z). The microscope is focused near the top electrode and has a ± 10-μm depth of focus. The top set of bright domain lines are visible and have a spacing of 31 μm or $\frac{1}{2}\lambda_t$. When the microscope is focused at the sample bottom, another set of bright domain lines is visible. Several dislocations in the domain pattern are visible as are many particles of dust, some badly out of focus.